Electrostatic model of coherent decay in a small spherical sample of two-level atoms of radially varying density

Richard Friedberg
Department of Physics, Columbia University, New York, New York 10027, USA

Jamal T. Manassah*
Department of Electrical Engineering, City College of New York, New York, New York 10031, USA

(Received 28 September 2011; published 28 March 2012)

We show that the decay rate and the frequency shift of the radiation modes from a small sphere of two-level atoms with varying radial density can be accurately obtained using an electrostatic model.

DOI: 10.1103/PhysRevA.85.033834 PACS number(s): 42.50.Nn

I. INTRODUCTION

We have recently presented [1] a study of coherent radiative emission from a small cloud (radius $\ll$ resonant wavelength) of identical two-level atoms, with spherical symmetry but strong radial variation of density. The purpose of this was to explore the relevance, to a small sample, of the Dicke picture [2] of coherent decay. In this picture, the atoms, if prepared in a completely symmetric state (analogous to a set of classical dipoles oscillating synchronously at the resonance frequency), will remain synchronous as the decay progresses, and the excitation will die out exponentially and uniformly throughout the sample.

The analysis of Ref. [2], however, is based only on the radiative reaction of the dipoles to each other's field, and ignores the frequency shifts [3] caused by the same field. These shifts are much larger, at short distance, than the cooperative decay rate, and in general should vary strongly within a small sample; therefore [4,5], the dipoles should dephase long before a significant fraction of the energy has been radiated.

An exception to the last statement is a spheroidal sample of uniform density. Here a well-known theorem of electrostatics tells us that a uniform polarization produces a uniform internal field, so that the Dicke picture is maintained in the small-sample limit [6]; see also Sec. II of Ref. [7] and Sec. VIII of Ref. [8].

The purpose of Ref. [1] was to show by explicit calculation that this exception no longer holds in a sphere with strongly varying atomic density. We studied two configurations: "shell-plus-hollow" consisting of a spherical shell of arbitrary thickness and uniform density surrounding a spherical hollow with no matter, and "shell-plus-core" in which there is an additional spherical core, of the same density as the shell, centered within the hollow. For each configuration, we set up the Maxwell and linearized Bloch equations governing time evolution in the regime of weak excitation (nearly all atoms in the ground state). For a sphere of arbitrary radius, these equations admit an eigenmode analysis in which the eigenfunctions involve spherical Bessel and Neuman functions. We confined ourselves to modes of angular index 1 (dipole symmetry) since we are interested in an initial state of uniform polarization. We studied the eigenmodes numerically for a certain small radius ($k_0 R = 0.05$, where $2\pi/k_0$ is the resonant wave number and R is the outermost radius) and found that the decomposition of the initial state is dominated by those modes of long ($\gg 2\pi/k_0$) wavelength, of which there are only two for the shell-plus-hollow and three for the shell-plus-core configuration.

The real and imaginary parts of the eigenvalues gave the radiation rates and frequency shifts of the respective modes. These quantities, as well as the relative contribution of each mode to the initial state, were calculated for a variety of assignments of the internal radii.

Although the methods of Ref. [1] are in principle applicable to any value of $k_0 R$, the numerical algorithms used become unreliable when $k_0 R$ is extremely small. Therefore, we carried out the calculations at $k_0 R = 0.05$. We also obtained the analytical limiting results as $k_0 R \to 0$ for the decay rate and frequency shift of the modes for the shell-plus-hollow configuration by performing a double series expansion of a characteristic fourth-order determinant (see the Appendix of Ref. [1]), which is a physically opaque procedure at best. In the present paper, we develop a different method by which the exact limit of all quantities of interest at $k_0 R \to 0$ is obtained analytically and transparently. Essentially, the idea is to put $k_0 R \to 0$ in Maxwell's equation from the start, so that one has merely an electrostatic problem. The resulting equations have no transcendental functions and can be solved by hand.

The Lienard-Wiechert potential for a small separation distance between two dipoles can be approximated by the expression

$$W(\Re) = \frac{\vec{p}_i \circ \vec{p}_j - 3\,\vec{p}_i \circ \hat{\Re}\,\vec{p}_j \circ \hat{\Re}}{\Re^3} - \frac{k_0^2(\vec{p}_i \circ \vec{p}_j + \vec{p}_i \circ \hat{\Re}\,\vec{p}_j \circ \hat{\Re})}{2\,\Re} - \frac{2}{3}\,i\,k_0^3\,\vec{p}_i \circ \vec{p}_j. \tag{1.1}$$

Our strategy will be, first, to replace (1.1) by its leading term. This causes each eigenmode to be described as an electrostatic boundary value problem with a dielectric constant related to the temporal eigenvalue. The problem turns out to be insoluble except for a small number of values of the dielectric constant. These determine the eigenmodes of the important modes. Since the electrostatic interaction is real, the dielectric constant in each mode is real, and hence the eigenvalues are purely

*jmanassah@gmail.com

imaginary. Thus this treatment yields frequency shifts but no decay rates.

The leading-order decay rate comes from the (imaginary) third term of Eq. (1.1) and is therefore $O((k_0R)^3)$ smaller than the frequency shifts, which, in turn, are of the order of the Lorentz shift ω_L. Thus, in the limit $k_0R \to 0$, the system does not decay in the time scale of $1/\omega_L$. Of interest, however, is the decay rate on the Dicke time scale $1/[\omega_L(k_0R)^3]$. This is found *exactly* by including the term in $-\frac{2}{3}ik_0^3$ to the leading order.

The way to do this is to find the expectation value of this term (viewed as an operator on the polarization distribution) in the "state" (to borrow quantum mechanical language) defined by the eigenmode already determined by electrostatics. The perturbation of the eigenmode by the second and third terms of Eq. (1.1) is of the order of $(k_0R)^2$ and can be neglected since it would affect the decay rate only to the order higher than $\omega_L(k_0R)^3$. The ratio of the decay rate to $\omega_L\,(k_0R)^3$ is a finite quantity in the limit $(k_0R)^3 \to 0$, and is found exactly by the method described here. Its analytic expression for both modes of the shell-plus-hollow configuration agrees exactly with that found in the Appendix of Ref. [1]. (An analogous calculation for the shell-plus-core configuration was not attempted in Ref. [1].)

Having found the eigenfunctions (field and polarization density) for each mode and the frequency shift and decay rate for each, we combine them to form the initial state (uniform polarization in the occupied volume) and follow its time development on both the Lorentz scale $1/\omega_L$, where ω_L is the Lorentz shift, and the Dicke scale $1/[\omega_L(k_0R)^3]$. On the Dicke scale, we obtain formulas for the overall emission rate and for $P - P^+$, which is the probability of excitation orthogonal to the initial state, as functions of time. These both turn out substantially different from the Dicke predictions. We also study the polarization density distribution in each eigenmode and make physical observations not brought out in [1].

In Sec. II, we give the fundamental equations as in [1], but modified for the limit $k_0R \to 0$. In Sec. III, we consider the shell-plus-hollow configuration. We set up the linear equation governing the change of the polarization, and find that its eigenmodes are given, to the leading order in k_0R, by solving an electrostatic problem with no source but an artificially chosen dielectric constant that satisfies a quadratic equation whose roots determine the frequency eigenvalues of two modes. Each mode is characterized by a nonuniform polarization. The initial state of the uniform polarization is resolved into the two modes, which dephase and rephase periodically in a time on the Lorentz scale. We then compute the expectation value of the imaginary part of Eq. (1.1) in each mode, and find analytical formulas for the overall emission rate, as well as the probability of excitation orthogonal to the symmetric state, as a function of time on the Dicke scale.

In Sec. IV, we let the center of the sphere belong to the occupied portion so that the atoms belong to an inner core and an outer shell, with a gap in between. (This problem, in which the initial excitation is the same for all atoms, must not be confused with that of Sec. VII in Ref. [7], in which the atomic density is uniform but the initial excitation is not.) The modes are now three in number. One mode is quasiuniform, with the polarization constant throughout the shell but weaker than in the core; its frequency is the same as that of the uniform sphere. The other two modes resemble those found in Sec. II. The eigenvalues and eigenfunctions are all given analytically, and the frequency shifts and decay rates are studied as for the first configuration.

In Sec. V, we summarize our results. Next, in the first two Appendices, we derive some features of the shell-plus-core configuration that were stated without proof in the text. Appendix C investigates a third configuration, in which the core and shell have different densities but there is no gap.

II. FUNDAMENTAL EQUATIONS

As in Ref. [1], we start with the Maxwell and linearized Bloch equations describing coherent decay from weak excitation. In an eigenmode where the electric field $\vec{\mathbf{E}}(\vec{r},t)$ and polarization $\vec{\mathbf{P}}(\vec{r},t)$ vary temporally as $\exp(-i\omega t)$, with $\omega = \omega_0 - \omega_L - i\lambda$, and λ being a complex quantity pertaining to the mode, we obtained (Eqs. (2.4) and (2.5) in Ref. [1])

$$\vec{\mathbf{P}}(\vec{r}) = -\frac{n\wp^2}{\hbar\lambda}\vec{\mathbf{E}}(\vec{r}) \text{ (occupied region)}, \tag{2.1}$$

and

$$\vec{\mathbf{E}}(\vec{r}) + \frac{4}{3}\pi\,\vec{\mathbf{P}}(\vec{r}) = -\int d^3\vec{r}'\,\exp(ik_0\Re) \times\left\{\left(\frac{1}{\Re^3} - i\frac{k_0}{\Re^2}\right)[\vec{\mathbf{P}}(\vec{r}') - 3\hat{\Re}\hat{\Re}\circ\vec{\mathbf{P}}(\vec{r}')] - \frac{k_0^2}{\Re}\,[\vec{\mathbf{P}}(\vec{r}') - \hat{\Re}\hat{\Re}\circ\vec{\mathbf{P}}(\vec{r}')]\right\}. \tag{2.2}$$

(We write $\vec{\Re} = \Re\hat{\Re} = \vec{r} - \vec{r}'$ and suppress the argument t. $\wp$ is the electric dipole matrix element and n is the atomic number density throughout the occupied region.)

Here we shall replace the integrand in Eq. (2.2) by its leading (electrostatic) term, corresponding to the first term in Eq. (1.1):

$$\vec{\mathbf{E}}(\vec{r}) + \frac{4}{3}\pi\vec{\mathbf{P}}(\vec{r}) = -\int d^3\vec{r}'\exp(ik_0\Re) \times\left\{\frac{1}{\Re^3}[\vec{\mathbf{P}}(\vec{r}') - 3\hat{\Re}\hat{\Re}\circ\vec{\mathbf{P}}(\vec{r}')]\right\}. \tag{2.3}$$

As in Ref. [1], the integral around the singularity is to be taken spherically, yielding the Clausius-Mossotti "local-field correction" exactly equal to the term $\frac{4}{3}\pi\vec{\mathbf{P}}(\vec{r})$ on the left. Thus, (2.3) reduces as in electrostatics to the pair of equations

$$\vec{\mathbf{E}} = -\vec{\nabla}V \tag{2.4}$$

and

$$\vec{\nabla}\circ(\vec{\mathbf{E}} + 4\pi\vec{\mathbf{P}}) = 0. \tag{2.5}$$

At the same time, Eq. (2.1) can be written as $\vec{\mathbf{P}} = \chi_s\vec{\mathbf{E}}$, where s labels the mode and

$$\chi_s = (1/i\lambda_s)(n\wp^2/\hbar), \tag{2.6}$$

and (2.5) becomes

$$\vec{\nabla}\circ(\varepsilon\,\vec{\mathbf{E}}) = 0, \tag{2.7}$$

where (for mode s) ε takes the values

$$\varepsilon_s = 1 + 4\pi\chi_s \tag{2.8}$$

in the occupied region, and 1 in the unoccupied region.

III. SHELL-PLUS-HOLLOW CONFIGURATION

In our geometry, Eqs. (2.4) and (2.7) lead to solutions of the form

$$V = \mathcal{A}_2 R^3 \cos(\theta)/r^2, \quad r > R, \tag{3.1}$$

$$V = \mathcal{B}_1 r\,\cos(\theta) + \mathcal{B}_2 R^3 \cos(\theta)/r^2, \quad \beta R < r \leqslant R, \tag{3.2}$$

$$V = \mathcal{C}_1 r\,\cos(\theta), \quad r \leqslant \beta R. \tag{3.3}$$

Since V and $\varepsilon\partial V/\partial r$ must be continuous at the boundaries, we have

$$\mathcal{A}_2 = \mathcal{B}_1 + \mathcal{B}_2, \tag{3.4a}$$

$$-2\,\mathcal{A}_2 = \varepsilon_s\,(\mathcal{B}_1 - 2\,\mathcal{B}_2), \tag{3.4b}$$

$$\mathcal{C}_1 = \mathcal{B}_1 + \mathcal{B}_2/\beta^3, \tag{3.5a}$$

$$\mathcal{C}_1 = \varepsilon_s\,(\mathcal{B}_1 - 2\,\mathcal{B}_2/\beta^3), \tag{3.5b}$$

and hence

$$(\varepsilon_s + 2)\,\mathcal{B}_1 = 2\,(\varepsilon_s - 1)\,\mathcal{B}_2, \tag{3.6}$$

$$(\varepsilon_s - 1)\,\mathcal{B}_1 = (2\,\varepsilon_s + 1)\,\mathcal{B}_2/\beta^3. \tag{3.7}$$

From this we find the equation determining ε_s:

$$(\varepsilon_s + 2)\,(2\,\varepsilon_s + 1) = 2\,(\varepsilon_s - 1)^2\beta^3, \tag{3.8}$$

and since (2.6) can be written

$$\varepsilon_s = 1 + (C/i\lambda_s), \tag{3.9}$$

where $C = \frac{4\pi n\wp^2}{\hbar} = 3\omega_L$, we have the eigenvalue equation $[3 + (C/i\lambda_s)][3 + 2\,(C/i\lambda_s)] = 2\,\beta^3(C/i\lambda_s)$, or, if we put $\lambda_s = iC\mu_s$, then

$$(3\mu_s - 1)(3\mu_s - 2) = 2\beta^3, \tag{3.10}$$

of which the two roots (taking $\pm$ for the values of s) are

$$\mu_\pm = \tfrac{1}{2} \pm \tfrac{1}{6}\sqrt{1 + 8\beta^3}. \tag{3.11}$$

As $\beta \to 0$, the roots approach 2/3 and 1/3; as $\beta \to 1$, they approach 1 and 0. The sum of the two roots is always 1. (If the Lorentz shift is included, then the total shift for each mode, with overall sign convention as in Ref. [9], is $-[\mathrm{Im}(\lambda) - \omega_L] = -C\,(\mu - \frac{1}{3})$.)

The distribution of polarization in each of the two modes depends on the ratio $\mathcal{B}_1/\mathcal{B}_2$; $\mathcal{B}_1$ is the coefficient of uniform polarization within the occupied region, and $\mathcal{B}_2$ is the coefficient of a distribution resembling a point dipole field. Using either (3.6) or (3.7), and $\varepsilon_s = 1 - (1/\mu_s)$ from Eq. (3.9), we find using (3.10) that

$$\mathcal{B}_1^\pm/\mathcal{B}_2^\pm = (1 \mp \sqrt{1 + 8\beta^3})/2\beta^3. \tag{3.12}$$

[The superscript $\pm$ refers to the choice of mode s, as in Eq. (3.11).]

As $\beta \to 0$, the lower solution of Eq. (3.10) ($\varepsilon_- \to -2, \mu_- \to \frac{1}{3}$) becomes dominated by $\mathcal{B}_1$. When $\beta = 0$, this solution becomes the configuration of uniform polarization discussed in Sec. II of Ref. [7]. The upper solution ($\varepsilon_+ \to -\frac{1}{2}, \mu_+ \to \frac{2}{3}$) yields $\mathcal{B}_1/\mathcal{B}_2 \to -2$; in this solution, the point dipole configuration dominates near the inner surface of the shell, and when $\beta = 0$, the solution no longer exists because of the singularity at the origin.

Until now, the normalization in each mode has been arbitrary. We now wish to fix this normalization so as to reproduce, for given β, the condition of uniform polarization density assumed at initial time $t = 0$. Let us write the actual polarization in the occupied region at $t = 0$ as

$$\vec{\mathbf{P}}(\vec{r},0) = \vec{\mathbf{P}}_+(\vec{r},0) + \vec{\mathbf{P}}_-(\vec{r},0) = -\chi_+\,\vec{\nabla}V_+(\vec{r}) - \chi_-\,\vec{\nabla}V_-(\vec{r}), \tag{3.13}$$

where $V_\pm$ are the two solutions of Eqs. (2.4) and (2.7) corresponding to the two modes, each normalized in a way to be determined. Then we have, in the occupied region,

$$\vec{\mathbf{P}}(\vec{r},t=0) = -\vec{\nabla}\Big[(\chi_+\mathcal{B}_1^+ + \chi_-\mathcal{B}_1^-)\,r\,\cos\theta + (\chi_+\mathcal{B}_2^+ + \chi_-\mathcal{B}_2^-)\frac{\cos\theta}{r^2}\Big]. \tag{3.14}$$

However, we want $\vec{\mathbf{P}}(\vec{r},0)$ to be equal to $P_0\hat{e}_z = P_0\vec{\nabla}(r\cos(\theta))$ for some P_0 independent of $\vec{r}$. This requires

$$\chi_+\mathcal{B}_1^+ + \chi_-\mathcal{B}_1^- = -P_0, \tag{3.15}$$

$$\chi_+\mathcal{B}_2^+ + \chi_-\mathcal{B}_2^- = 0. \tag{3.16}$$

From Eq. (3.16), we have

$$\frac{\chi_+\mathcal{B}_2^+}{\chi_-\mathcal{B}_2^-} = -1, \tag{3.17}$$

and hence from Eq. (3.12),

$$\frac{\chi_+\mathcal{B}_1^+}{\chi_-\mathcal{B}_1^-} = -\frac{(1 - \sqrt{1 + 8\,\beta^3})}{(1 + \sqrt{1 + 8\,\beta^3})}. \tag{3.18}$$

Therefore, from Eq. (3.15),

$$\chi_\pm B_1^\pm = -\frac{1}{2}P_0\left(1 \mp \frac{1}{\sqrt{1 + 8\,\beta^3}}\right), \tag{3.19}$$

and applying (3.12) again,

$$\chi_\pm\mathcal{B}_2^\pm = \pm P_0\frac{\beta^3}{\sqrt{1 + 8\beta^3}}. \tag{3.20}$$

Note the distinction between $\sqrt{1 + 8\beta^3}$ and $1/\sqrt{1 + 8\beta^3}$.

We can now study the time evolution of the polarization distribution. Let us put

$$\vec{\mathbf{P}}(r,t) = \vec{\nabla}\,[F_1(t)\,r\,\cos(\theta) + F_2(t)\,R^3\,\cos(\theta)/r^2] = F_1(t)\,\hat{e}_z + F_2(t)\,(R/r)^3[-2\,\cos(\theta)\,\hat{e}_r - \sin(\theta)\,\hat{e}_\theta]. \tag{3.21}$$

Then,

$$F_1(t) = -\chi_+\mathcal{B}_1^+\exp(-\lambda_+ t) - \chi_-\mathcal{B}_1^-\exp(-\lambda_- t), \tag{3.22}$$

$$F_2(t) = -\chi_+\mathcal{B}_2^+\exp(-\lambda_+ t) + \chi_-\mathcal{B}_2^-\exp(-\lambda_- t), \tag{3.23}$$

where the factors $\chi\mathcal{B}$ are given by Eq. (3.19) and (3.20). [We continue to omit the Lorentz shift which, as previously pointed out, would supply an overall factor $\exp(i\omega_L t) = \exp(iCt/3)$.]

So far we have considered λ_s to be completely imaginary on the basis of Eqs. (2.2) and (2.3), but we shall presently introduce the idea that λ_s has a small real part proportional to k_0^3, which we have so far taken to be zero.

Of particular interest to us is the quantity $P - P^+$, where P denotes the fraction of energy remaining in the atoms (not radiated), and P^+ is the fractional probability that the atoms are excited and phased to radiate forward as at time $t = 0$ (i.e., proportional to the squared magnitude of the forward emission amplitude). In our continuum notation, we have

$$P(t) = \frac{\int d^3\vec{r}\,|\vec{P}(\vec{r},t)|^2}{\int d^3\vec{r}\,|\vec{P}(\vec{r},0)|^2} = \frac{|F_1(t)|^2 + (2/\beta^3)|F_2(t)|^2}{P_0^2}, \tag{3.24}$$

$$P^+(t) = \left|\frac{\int d^3\vec{r}\,\vec{P}(\vec{r},t)\circ\hat{e}_z}{\int d^3\vec{r}\,\vec{P}(\vec{r},0)\circ\hat{e}_z}\right|^2 = \frac{|F_1(t)|^2}{P_0^2}. \tag{3.25}$$

Combining (3.24) and (3.25), we have

$$P(t) - P^+(t) = (2/\beta^3)\,\frac{|F_2(t)|^2}{P_0^2}, \tag{3.26}$$

and from Eq. (3.23) with Eqs. (3.16) and (3.20), disregarding the small real part of λ,

$$P(t) - P^+(t) = \frac{2\,\beta^3}{1 + 8\,\beta^3}\,[2 - 2\,\cos(\delta\, t)], \tag{3.27}$$

where

$$\delta = \mathrm{Im}(\lambda_+) - \mathrm{Im}(\lambda_-) = C(\mu_+ - \mu_-) = (C/3)\,\sqrt{1 + 8\,\beta^3}. \tag{3.28}$$

$P - P^+$ gives the cumulative fraction of nonradiative transfer (NRT) [10], that is, the probability at time t that the atoms, initially in a coherent state of single excitation corresponding to uniform polarization, are now in a state of single excitation orthogonal to the uniform one. From Eq. (3.27), we see that if $\beta = 0$, then this quantity is zero at all times, which is in agreement with the finding of Ref. [4] for the uniformly populated sphere with no internal cavity. For nonzero β, we see that $P - P^+$ is initially zero, but thereafter oscillates between 0 and $8\beta^3/(1 + 8\beta^3)$.

The above description applies in a time scale of the order of C^{-1} (the "fast scale"), which governs the oscillations. On this scale, the real part of λ_s can be neglected. Let us now take it into account. This quantity can be written for each s as

$$\mathrm{Re}(\lambda_s) = q_s\lambda_D, \tag{3.29}$$

where the dimensionless coefficients q_s are $O(1)$, and

$$\lambda_D = N\gamma_1/2, \tag{3.30}$$

where $\gamma_1 = \frac{4}{3}\,(\wp^2 k_0^3/\hbar)$ is the decay rate of the probability of excitation of the isolated atom, and $N = (4/3)\,\pi\,R^3(1 - \beta^3)\,n$ is the number of atoms. Thus,

$$\begin{aligned}\lambda_D &= \tfrac{1}{2}(4/3)^2\pi n\wp^2(k_0R)^3(1 - \beta^3)/\hbar \\ &= (2/9)C(k_0R)^3(1 - \beta^3).\end{aligned} \tag{3.31}$$

The factor $(k_0R)^3$ causes λ_D to vanish on the scale of C. (Recall that $C = 3\omega_L$.)

Including the decay factors, Eq. (3.27) should be replaced by

$$\begin{aligned}P(t) - P^+(t) = \frac{2\beta^3}{1 + 8\beta^3}\{&\exp[-2\mathrm{Re}(\lambda_+)t] + \exp[-2\mathrm{Re}(\lambda_-)t] \\ &- 2\exp[-\mathrm{Re}(\lambda_+ + \lambda_-)t]\cos(\delta t)\}.\end{aligned} \tag{3.32}$$

Let us now look at things as seen on a time scale of the order of $(\lambda_D)^{-1}$ (the "slow scale"). The exponents in Eq. (3.32) contain terms $-\mathrm{Re}(\lambda_\pm t)$, which are of the order $O(1)$ on the slow scale. Furthermore, δt is essentially infinite on the slow scale; that is, the oscillations in Eq. (3.32) are infinitely fast so that we see only their average. Thus, the factor $\cos(\delta t)$ is replaced by zero. This means that on the slow scale, the value of $P - P^+$ is surprisingly already nonzero ($=\frac{4\beta^3}{1+8\beta^3}$) at what appears to be the initial time. Putting $\mathrm{Re}(\lambda_\pm)$ in terms of λ_D by Eq. (3.29), we thus replace (3.32) by

$$\begin{aligned}&P(t) - P^+(t) \\ &= \frac{2\,\beta^3}{1 + 8\,\beta^3}\,[\exp(-2q_+\lambda_D t) + \exp(-2q_-\lambda_D t)].\end{aligned} \tag{3.33}$$

Let us now study P. When (3.24) is evaluated by means of using (3.22), (3.23), and (3.15), (3.16), some surprising simplifications lead to

$$\begin{aligned}P(t) = \frac{1}{2}\Bigg[&\left(1 - \frac{1}{\sqrt{1 + 8\beta^3}}\right)\exp(-2q_+\lambda_D t) \\ &+ \left(1 + \frac{1}{\sqrt{1 + 8\beta^3}}\right)\exp(-2q_-\lambda_D t)\Bigg].\end{aligned} \tag{3.34}$$

Note that the terms involving $\cos(\delta t)$ have cancelled. Thus, P does not undergo fast oscillation; the oscillations seen in Eqs. (3.27) and (3.32) are entirely due to P^+. This is physically expected, since energy once radiated (lost to P) cannot return to the system.

Now we must calculate $q_s = \mathrm{Re}(\lambda_s)/\lambda_D$. As is well known, the right-hand side of Eq. (2.2) is only the leading term (in powers of k_0R) of a complex expression,

$$\begin{aligned}\exp(i\,k_0\,\Re)\Bigg\{&[3\,\vec{P}(\vec{r}\,')\circ\hat{\Re}\,\hat{\Re} - \vec{P}(\vec{r}\,')]\left(\frac{1 - i\,k_0\,\Re}{\Re^3}\right) \\ &- \frac{k_0^2}{\Re}\,[\vec{P}(\vec{r}\,')\circ\hat{\Re}\,\hat{\Re} - \vec{P}(\vec{r}\,')]\Bigg\},\end{aligned} \tag{3.35}$$

of which the imaginary part has the leading term $(2/3)\,k_0^3$ independent of $\Re$. (This independence is the foundation for the Dicke picture for the uniformly dense small sphere.) This small imaginary part does not affect noticeably the eigenfunctions of our system, but it gives rise perturbatively to the real part of the eigenvalues. Thus,

$$\begin{aligned}\mathrm{Re}(\lambda_s) &= \left(\frac{n\,\wp^2}{\hbar}\right)\left(\frac{2}{3}\,k_0^3\right)\frac{\int d^3\vec{r}\int d^3\vec{r}\,'\,\vec{P}_s(\vec{r})\circ\vec{P}_s(\vec{r}\,')}{\int d^3\vec{r}\,|\vec{P}_s(\vec{r})\,|^2} \\ &= \left(\frac{n\,\wp^2}{\hbar}\right)\left(\frac{2}{3}\,k_0^3\right)\frac{\left|\int d^3\vec{r}\,\vec{P}_s(\vec{r})\right|^2}{\int d^3\vec{r}\,|\vec{P}_s(\vec{r})\,|^2},\end{aligned} \tag{3.36}$$

while

$$\lambda_D = \left(\frac{n\,\wp^2}{\hbar}\right)\left(\frac{2}{3}\,k_0^3\right)\int d^3\vec{r}, \tag{3.37}$$

so that

$$\frac{\mathrm{Re}(\lambda_s)}{\lambda_D} = \frac{\left|\int d^3\vec{r}\ \vec{P}_s(\vec{r})\right|^2}{\int d^3\vec{r}\,|\vec{P}_s(\vec{r})|^2 \int d^3\vec{r}}, \tag{3.38}$$

where $\vec{\mathbf{P}}_s$ is the portion of Eq. (3.14) proportional to χ_s.

The integral of $\vec{\mathbf{P}}_s$ receives a contribution only from the part of Eq. (3.14) proportional to $\chi_s \mathcal{B}_1^s$, so that

$$q_s = \frac{\left(\mathcal{B}_1^s\right)^2}{\left(\mathcal{B}_1^s\right)^2 + (2/\beta^3)\left(\mathcal{B}_2^s\right)^2}. \tag{3.39}$$

Applying (3.12), we have

$$q_\pm = \frac{1+4\beta^3 \mp \sqrt{1+8\beta^3}}{1+8\beta^3 \mp \sqrt{1+8\beta^3}} = \frac{1}{2}\left(1 \mp \frac{1}{\sqrt{1+8\beta^3}}\right). \tag{3.40}$$

Finally, by comparing (3.40) to (3.34), we find curiously that

$$P(t) = \sum_s q_s\ \exp(-2\,q_s\lambda_D t), \tag{3.41}$$

and hence that the overall radiation rate, relative to the initial energy, is

$$-\frac{d}{\lambda_D dt}\,P(t) = 2\sum_s q_s^2\ \exp(-2\,q_s\lambda_D t), \tag{3.42}$$

with q_s given by Eq. (3.40).

A careful examination of the definitions shows that (3.41) implies another identity,

$$P^+(t) = \left|\sum_s q_s \exp(-\lambda_s t)\right|^2, \tag{3.43}$$

which can also be derived from Eq. (3.25) and the preceding equations.

IV. SHELL-PLUS-CORE CONFIGURATION

The methods of the preceding section can readily be generalized to a sphere with two occupied regions. We take the density of resonant atoms as n in regions II and IV, 0 in regions I and III, where

$$\text{I (outside)}: \ r > R, \tag{4.1}$$
$$\text{II (shell)}: R > r > \beta R, \tag{4.2}$$
$$\text{III (gap)}: \beta R > r > \gamma R, \tag{4.3}$$
$$\text{IV (core)}: \ \gamma R > r > 0. \tag{4.4}$$

The potential function is now given as

$$V = \mathcal{A}_2 R^3\cos(\theta)/r^2, \quad r > R, \tag{4.5}$$
$$V = \mathcal{B}_1 r\ \cos(\theta) + \mathcal{B}_2 R^3\cos(\theta)/r^2, \quad R > r > \beta R, \tag{4.6}$$
$$V = \mathcal{C}_1 r\ \cos(\theta) + \mathcal{C}_2 R^3\cos(\theta)/r^2, \quad \beta R > r > \gamma\, R, \tag{4.7}$$
$$V = \mathcal{D}_1 r\ \cos(\theta), \quad \gamma R > r > 0. \tag{4.8}$$

The boundary conditions are

$$\mathcal{A}_2 = \mathcal{B}_1 + \mathcal{B}_2, \tag{4.9a}$$
$$-2\,\mathcal{A}_2 = \varepsilon\,(\mathcal{B}_1 - 2\,\mathcal{B}_2), \tag{4.9b}$$
$$\mathcal{C}_1 + S_\beta \mathcal{C}_2 = \mathcal{B}_1 + S_\beta \mathcal{B}_2, \tag{4.10a}$$
$$\mathcal{C}_1 - 2\,S_\beta \mathcal{C}_2 = \varepsilon\,(\mathcal{B}_1 - 2S_\beta \mathcal{B}_2), \tag{4.10b}$$
$$\mathcal{C}_1 + S_\gamma \mathcal{C}_2 = \mathcal{D}_1, \tag{4.11a}$$
$$\mathcal{C}_1 - 2\,S_\gamma \mathcal{C}_2 = \varepsilon\,\mathcal{D}_1, \tag{4.11b}$$

where $S_\beta = (1/\beta^3)$ and $S_\gamma = (1/\gamma^3)$.

Eliminating $\mathcal{A}_2$ and $\mathcal{D}_1$, we find

$$\mathcal{B}_1 = 2(\varepsilon - 1)\mathcal{B}_0, \tag{4.12a}$$
$$\mathcal{B}_2 = (\varepsilon + 2)\mathcal{B}_0, \tag{4.12b}$$
$$\mathcal{C}_1 = (\varepsilon + 2)S_\gamma \mathcal{C}_0, \tag{4.13a}$$
$$\mathcal{C}_2 = -(\varepsilon - 1)\mathcal{C}_0, \tag{4.13b}$$

where

$$\mathcal{B}_0\{2(\varepsilon - 1) + (\varepsilon + 2)\,S_\beta\} = \mathcal{C}_0\{(\varepsilon + 2)\,S_\gamma - (\varepsilon - 1)\,S_\beta\}, \tag{4.14}$$

$$\varepsilon\mathcal{B}_0\{2(\varepsilon - 1) - 2(\varepsilon + 2)S_\beta\} = \mathcal{C}_0\{(\varepsilon + 2)S_\gamma + 2(\varepsilon - 1)S_\beta\}. \tag{4.15}$$

The secular equation for this homogeneous system is

$$M = \begin{vmatrix} 2(\varepsilon - 1) + (\varepsilon + 2)S_\beta & (\varepsilon + 2)S_\gamma - (\varepsilon - 1)S_\beta \\ \varepsilon[2(\varepsilon - 1) - 2(\varepsilon + 2)S_\beta] & (\varepsilon + 2)S_\gamma + 2(\varepsilon - 1)S_\beta \end{vmatrix} = 0. \tag{4.16}$$

The secular equation reduces to

$$M = (\varepsilon + 2)\big[2\big(-S_\gamma + S_\beta - S_\beta^2\big)(\varepsilon - 1)^2 + (\varepsilon + 2)(2\varepsilon - 1)S_\beta S_\gamma\big]. \tag{4.17}$$

The vanishing of the factor in the square bracket gives an equation identical to Eq. (3.4) except that β^3 is replaced by $\tilde{\beta}^3$:

$$\tilde{\beta}^3 = \frac{S_\gamma - S_\beta + S_\beta^2}{S_\beta S_\gamma} = \beta^3 - \gamma^3 + \frac{\gamma^3}{\beta^3} \tag{4.18}$$

Thus the secular equation, expressed in terms of μ, admits one fixed root (independent of both β and γ) and two other roots having the same functional form as those of the single shell configuration, but with β replaced by $\tilde{\beta}$:

$$\mu_0 = \tfrac{1}{3}, \quad \mu_\pm = \tfrac{1}{2} \pm \tfrac{1}{6}\sqrt{1+8\tilde{\beta}^3}. \tag{4.19}$$

The three roots add to 4/3.

In the "fixed" solution $\mu_0 = 1/3$, $\varepsilon_0 = -2$, we see from Eqs. (4.12) and (4.13) that $\mathcal{B}_2 = \mathcal{C}_1 = 0$; therefore, the field has point dipole behavior in the "gap," and uniform behavior, along with the polarization, in the "shell." This solution may be called quasiuniform, in that the polarization is uniform within each occupied region. The nonuniformity consists in the inequality of $\mathcal{D}_1$ to $\mathcal{B}_1$; putting $\mathcal{C}_1 = 0$ in the original boundary conditions, we find

$$\mathcal{B}_1 = (\gamma^3/\beta^3)\mathcal{D}_1. \tag{4.20}$$

When $\gamma = \beta$ (no gap), this mode becomes uniform and completely describes the initial state as in Sec. II of Ref. [7]. When $\gamma = 0$ (no core), the fixed solution ceases to exist because of the singularity in the origin ($\mathcal{C}_2 \neq 0$).

The two unfixed modes do not become singular when $\gamma = 0$ because $\mathcal{C}_2/\mathcal{C}_1$ vanishes by Eq. (4.13). They become the two modes of Sec. II since then $\tilde{\beta}^3 = \beta^3$.

For general γ and β, the real part of λ can be derived from Eq. (3.29) and (3.38). The result is like (3.39), but with shell and core contributions weighted by volume:

$$q_s = \frac{\left[(1-\beta^3)\mathcal{B}_1^s + \gamma^3 \mathcal{D}_1^s\right]^2}{\left\{\left[\left(\mathcal{B}_1^s\right)^2 + 2\beta^{-3}\left(\mathcal{B}_2^s\right)^2\right](1-\beta^3) + \gamma^3\left(\mathcal{D}_1^s\right)^2\right\}(1-\beta^3+\gamma^3)} \tag{4.21}$$

For the fixed mode, using (4.20) and dropping B_2, this becomes

$$q_0 = \frac{[(1-\beta^3)\gamma^3 + \gamma^3\beta^3]^2}{[(1-\beta^3)\gamma^6 + \gamma^3\beta^6](1-\beta^3+\gamma^3)} = \frac{\gamma^3}{(\gamma^3 - \beta^3\gamma^3 + \beta^6)(1-\beta^3+\gamma^3)} \tag{4.22}$$

For the unfixed modes, one obtains (see Appendix A)

$$\frac{\mathcal{B}_1^{\pm}}{\mathcal{D}_1^{\pm}} = \frac{1}{1-S_\beta}, \quad \frac{\mathcal{B}_2^{\pm}}{\mathcal{B}_1^{\pm}} = \frac{3\mu_\pm - 1}{2}. \tag{4.23}$$

On substituting (4.23) into Eq. (4.21) (Appendix B), the expressions for the $q_\pm$ simplify to

$$q_+ = \frac{2(1-\beta^3)(\beta^3-\gamma^3)^2}{3\beta^3(3\mu_+ - 1)(\mu_+ - \mu_-)(1-\beta^3+\gamma^3)}, \tag{4.24a}$$

$$q_- = \frac{2(1-\beta^3)(\beta^3-\gamma^3)^2}{3\beta^3(3\mu_- - 1)(\mu_- - \mu_+)(1-\beta^3+\gamma^3)}. \tag{4.24b}$$

To obtain the sum of the three q's, we use the identity

$$\frac{1}{(3\mu_+ - 1)3(\mu_+ - \mu_-)} + \frac{1}{(3\mu_- - 1)3(\mu_- - \mu_+)} = -\frac{1}{(3\mu_+ - 1)(3\mu_- - 1)}. \tag{4.25}$$

and putting $\mu_- = 1 - \mu_+$, the right-hand side becomes

$$\frac{1}{(3\mu_+ - 1)(3\mu_+ - 2)} = \frac{1}{2\tilde{\beta}^3} = \frac{1}{2}\frac{\beta^3}{\beta^6 - \beta^3\gamma^3 + \gamma^3}. \tag{4.26}$$

Hence,

$$q_+ + q_- = \frac{(1-\beta^3)(\beta^3-\gamma^3)^2}{(\gamma^3 - \beta^3\gamma^3 + \beta^6)(1-\beta^3+\gamma^3)}. \tag{4.27}$$

Combining with Eq. (4.22), we have

$$q_0 + q_+ + q_- = \frac{[\gamma^3 + (1-\beta^3)(\beta^3-\gamma^3)^2]}{(\gamma^3 - \beta^3\gamma^3 + \beta^6)(1-\beta^3+\gamma^3)}. \tag{4.28}$$

A straightforward expansion shows that the numerator and denominator are identical, hence, $\sum_s q_s = 1$, as expected.

The previously defined expressions for $P^+(t)$ and $P(t)$, namely, $P^+(t) = |\frac{\int d^3\vec{r}\,\vec{P}(\vec{r},t)\circ\hat{e}_z}{\int d^3\vec{r}\,\vec{P}(\vec{r},0)\circ\hat{e}_z}|^2$ and $P(t) = \frac{\int d^3\vec{r}\,|\vec{P}(\vec{r},t)|^2}{\int d^3\vec{r}\,|\vec{P}(\vec{r},0)|^2}$, can be written after some manipulation as

$$P^+(t) = \left|\sum_s q_s \exp(-\lambda_s t)\right|^2, \tag{4.29}$$

$$P(t) = \sum_s q_s \exp[-2\mathrm{Re}(\lambda_s)t]. \tag{4.30}$$

These identities, exactly parallel to Eqs. (3.41) and (3.43), emerge for each configuration in an apparently fortuitous way. We have no simple way of understanding them.

V. CONCLUSION

In Figs. 1 and 2, we graph Eqs. (3.33) and (3.42) on the Dicke time scale, for two values of β. In Fig 1, the Dicke picture would give $\mathbf{P} - \mathbf{P}^+ = 0$ for all time; in Fig 2, showing the emission rate, it would give exponential decay, which is shown for comparison. The departure from Dicke behavior is marked.

It was noted after Eq. (3.36) that the two values of q add to 1; that is, $\mathrm{Re}(\lambda_+) + \mathrm{Re}(\lambda_-) = \lambda_D$. This sum rule must hold for any geometry in the limit $k_0 R \to 0$, because the sum $\sum_s \mathrm{Re}(\lambda_s)$ is the trace of the operator whose expectation value is evaluated in (3.36), and this trace can be evaluated as a sum of diagonal elements, yielding (3.37). As shown by Eq. (4.28), this sum rule holds also in Sec. III. In Fig. 3, we plot the q_s's in the shell-plus-core configuration as a function of β for $\gamma = 0.2$, and note that the mode with $s = 0$ is not the dominant mode for all values of β.

We note, though, a second sum rule for $\mathrm{Im}(\lambda)$ that is not so robust or easily stated. For the uniform sphere (one mode), we have $\mu = 1/3$. For the shell-plus-hollow configuration (Sec. II, two modes), we have $\mu_+ + \mu_- = 1$. For the shell-plus-core configuration (Sec. III, three modes), we have $\mu_+ + \mu_- + \mu_0 = \frac{4}{3}$ (see Fig. 4). It can be shown that this pattern continues for any number of successive shells as long as all occupied regions have the same density. It appears that

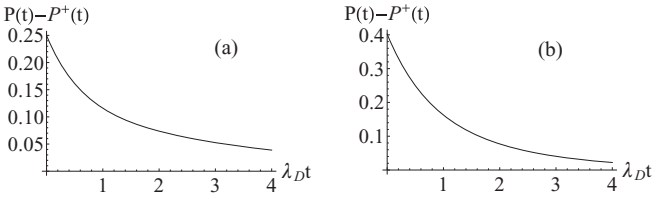

FIG. 1. The cumulative fraction $P - P^+$ of nonradiative transfer (NRT) is plotted as a function of the slow time for the shell-plus-hollow configuration. (a) $\beta = 0.5$; (b) $\beta = 0.8$. (This quantity is zero in the Dicke model.)

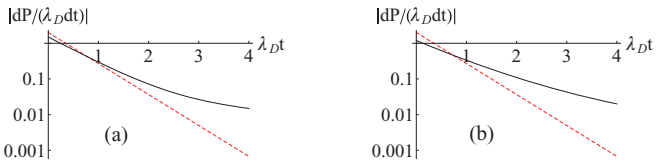

FIG. 2. (Color online) The radiation rate relative to the initial energy is plotted logarithmically as a function of the slow time for the shell-plus-hollow configuration. (a) $\beta = 0.5$; (b) $\beta = 0.8$. (Dashed line corresponds to Dicke's theory.)

the "trace" argument is disturbed, in the case of Im(λ), by the singularity of the operator at $\vec{r} = \vec{r}'$. But if all occupied regions have the same uniform density, then the disturbance can be localized to the interfaces between regions. A convex interface (filled region on the inside) contributes 1/3 to $\sum_s \mu_s$ (as in a uniform sphere in an empty world), whereas a concave interface (filled region on the outside) contributes 2/3 (as in an empty sphere in a uniformly filled world).

The surviving strength at any time of the original polarization distribution is given by $\mathbf{P}^+(t)$. On the fast time scale, if $\mathbf{P}^+$ is found in the two-mode problem from Eqs. (3.25) and (3.19), then its graph against $T = Ct$ is that of a simple sinusoidal function. In the shell-plus-core configuration, however, the three modes give rise to an interplay of incommensurate beat frequencies. Figure 5 illustrates this behavior.

In summary, the evolution of both the polarization and radiation rate, even in the limit $k_0 R \to 0$, shows marked deviations from Dicke behavior, both on the slow time scale $t \approx O(\lambda_D^{-1})$ and on the fast scale $t \approx O(C^{-1})$.

APPENDIX A

Here we derive Eq. (4.23) for the shell-plus-core configuration.

The ratio of $\mathcal{B}_1$ to $\mathcal{D}_1$ in any mode is obtained by combining (4.14) with Eqs. (4.11a) and (4.12a):

$$\frac{\mathcal{B}_1}{\mathcal{D}_1} = \frac{2(\varepsilon-1)}{3S_\gamma}\frac{(\varepsilon+2)S_\gamma - (\varepsilon-1)S_\beta}{2(\varepsilon-1)+(\varepsilon+2)S_\beta}. \tag{A1}$$

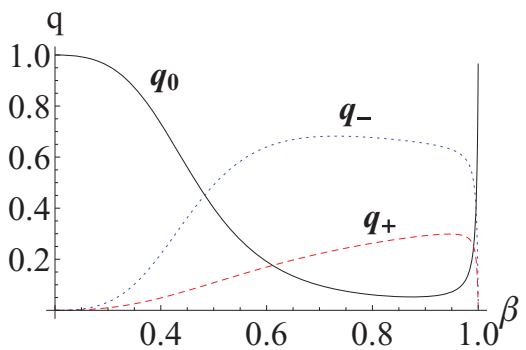

FIG. 3. (Color online) The ratio of the real part of the true eigenvalue to Dicke's value for the different modes for the shell-plus-core configuration are plotted as a function of β, with $\gamma = 0.2$.

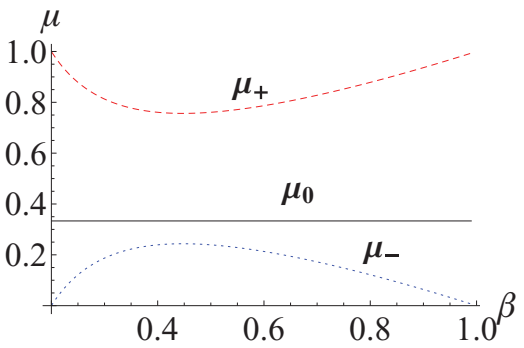

FIG. 4. (Color online) The normalized imaginary part of the eigenvalue [$\mu = \mathrm{Im}(\lambda)/C$] for the different modes for the shell-plus-core configuration is plotted as a function of β, with $\gamma = 0.2$.

Since $\varepsilon = 1 - \mu^{-1}$, $\frac{\varepsilon+2}{\varepsilon-1} = 1 - 3\mu$, (A1) is equivalent to

$$\frac{\mathcal{B}_1}{\mathcal{D}_1} = \frac{2}{-3S_\gamma\mu}\frac{S_\gamma(1-3\mu)-S_\beta}{2+S_\beta(1-3\mu)}. \tag{A2}$$

For the modes ±, we have also

$$(1-3\mu_s)(2-3\mu_s) = 2\tilde{\beta}^3 = 2\left(\beta^3 - \gamma^3 + \frac{\gamma^3}{\beta^3}\right), \tag{A3a}$$

or

$$3\mu_\pm(1-3\mu_\pm) = 2(1-3\mu_\pm) - 2\left(\beta^3 - \gamma^3 + \frac{\gamma^3}{\beta^3}\right). \tag{A3b}$$

Multiplying by $S_\beta S_\gamma$,

$$3\mu_\pm(1-3\mu_\pm)S_\beta S_\gamma = 2\left(S_\beta S_\gamma - S_\gamma + S_\beta - S_\beta^2\right) - 6\mu_\pm S_\beta S_\gamma, \tag{A4}$$

and adding $6\mu_\pm S_\gamma$ on both sides,

$$3\mu_\pm S_\gamma[2 + S_\beta(1-3\mu_\pm)] = -2\,(1-S_\beta)[S_\gamma(1-3\mu_\pm) - S_\beta]. \tag{A5}$$

Comparing (A5) to (A2), we see that

$$\frac{\mathcal{B}_1^\pm}{\mathcal{D}_1^\pm} = \frac{1}{(1-S_\beta)}. \tag{A6}$$

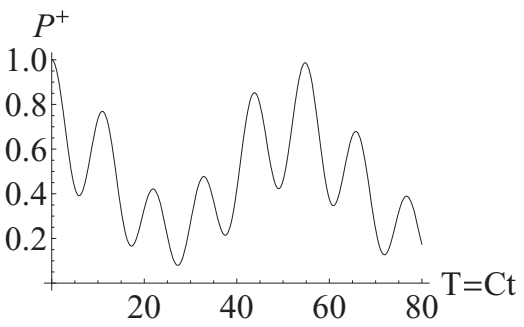

FIG. 5. $P^+(t)$ (proportional to the square magnitude of the forward emission amplitude) from an initially uniform polarization is plotted as a function of the fast normalized time ($T = Ct$) for the shell-plus-core configuration. $\beta = 0.6$ and $\gamma = 0.2$.

Also from (4.12a) and (4.12b),

$$\frac{\mathcal{B}_2^{\pm}}{\mathcal{B}_1^{\pm}} = \frac{(3\mu_{\pm}-1)}{2}. \tag{A7}$$

Thus (4.23) is confirmed.

APPENDIX B

We seek a formula for $q_{\pm}$ in the shell-plus-core configuration. Substituting (4.23) into (4.21), we have (remembering that $S_\beta = 1/\beta^3$)

$$\begin{aligned} q_{\pm} &= \frac{\left[(1-\beta^3)+\gamma^3(1-S_\beta)\right]^2}{\left\{(1-\beta^3)\left[1+2\,S_\beta\left(\frac{3\,\mu_{\pm}-1}{2}\right)^2\right]+\gamma^3(1-S_\beta)^2\right\}(1-\beta^3+\gamma^3)} \\ &= \frac{(1-S_\beta)^2(\beta^3-\gamma^3)^2}{-(1-S_\beta)\left\{\beta^3\left[1+\frac{1}{2}\,S_\beta\,(3\,\mu_{\pm}-1)^2\right]-\gamma^3(1-S_\beta)\right\}(1-\beta^3+\gamma^3)} \\ &= \frac{-(1-S_\beta)\;(\beta^3-\gamma^3)^2}{\left[\beta^3-\gamma^3+\frac{\gamma^3}{\beta^3}+\frac{1}{2}\,(3\,\mu_{\pm}-1)^2\right](1-\beta^3+\gamma^3)}\,. \end{aligned} \tag{B1}$$

Since

$$\beta^3-\gamma^3+\frac{\gamma^3}{\beta^3} = \tilde{\beta}^3 = \frac{1}{2}(3\mu_{\pm}-1)(3\mu_{\pm}-2), \tag{B2}$$

the square bracket in the denominator of Eq. (B1) is

$$\begin{aligned} &\tfrac{1}{2}(3\mu_{\pm}-1)(3\mu_{\pm}-2)+\tfrac{1}{2}(3\mu_{\pm}-1)^2 \\ &\quad = \tfrac{1}{2}(3\mu_{\pm}-1)(6\mu_{\pm}-3) = \tfrac{3}{2}(3\mu_{\pm}-1)(\mu_{\pm}-\mu_{\mp}) \end{aligned} \tag{B3}$$

where we have used $\mu_{\pm}+\mu_{\mp}=1$. Therefore,

$$q_{\pm} = \frac{2(S_{\beta}-1)(\beta^3-\gamma^3)^2}{3(3\mu_{\pm}-1)(\mu_{\pm}-\mu_{\mp})(1-\beta^3+\gamma^3)} \tag{B4}$$

Thus Eq. (4.24) is confirmed.

APPENDIX C

In this Appendix, we shall compute the eigenvalues for the shell-plus-shell configuration. In this configuration, the sphere is divided into two shells, both filled with the active atoms but where the density in the inside shell is ζn, and is n in the outer shell, where $0<\zeta<1$. There is no hollow part. The potential is given by Eqs. (3.1)–(3.3), but the dielectric constant in the region $r<\beta R$ is no longer 1. Superscripts b and c will be used, respectively, for the outer shell, $\beta R<r<R$, and the inner shell, $r<\beta R$.

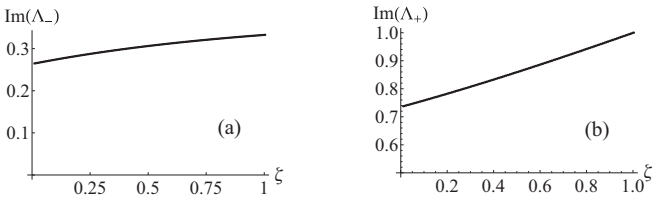

FIG. 6. Im(Λ) is plotted, for the two modes, as a function of the relative densityζ in the two shells in the shell-shell configuration. $\beta = 0.5$. Analytic result, for $k_0R=0$, from Appendix C superimposed on a numerical curve for $k_0R=0.05$.

The boundary conditions corresponding to Eqs. (3.4) and (3.5) become

$$\mathcal{A}_2 = \mathcal{B}_1+\mathcal{B}_2, \tag{C1a}$$

$$-2\mathcal{A}_2 = \varepsilon_s^{(b)}(\mathcal{B}_1-2\mathcal{B}_2), \tag{C1b}$$

$$\mathcal{C}_1 = \mathcal{B}_1+\mathcal{B}_2/\beta^3, \tag{C2a}$$

$$\varepsilon_s^{(c)}\mathcal{C}_1 = \varepsilon_s^{(b)}(\mathcal{B}_1-2\mathcal{B}_2/\beta^3), \tag{C2b}$$

and hence

$$\left(\varepsilon_s^{(b)}+2\right)\mathcal{B}_1 = 2\left(\varepsilon_s^{(b)}-1\right)\mathcal{B}_2, \tag{C3}$$

$$\left(\varepsilon_s^{(b)}-\varepsilon_s^{(c)}\right)\mathcal{B}_1 = \left(2\varepsilon_s^{(b)}+\varepsilon_s^{(c)}\right)\mathcal{B}_2/\beta^3. \tag{C4}$$

The solvability condition reduces to

$$\left(\varepsilon_s^{(b)}+2\right)\left(2\varepsilon_s^{(b)}+\varepsilon_s^{(c)}\right)-2\left(\varepsilon_s^{(b)}-1\right)\left(\varepsilon_s^{(b)}-\varepsilon_s^{(c)}\right)\beta^3 = 0. \tag{C5}$$

The dielectric constants in the two regions are given by

$$\varepsilon_s^{(c)} = 1+\frac{\zeta C}{i\lambda_s}, \tag{C6}$$

$$\varepsilon_s^{(b)} = 1+\frac{C}{i\lambda_s}, \tag{C7}$$

where $\lambda_s = iC\mu_s$ and $C = \frac{4\pi n\wp^2}{\hbar}$.

The characteristic equation reduces to

$$(3\mu_s-1)[3\mu_s-(2+\zeta)] = 2(1-\zeta)\beta^3. \tag{C8}$$

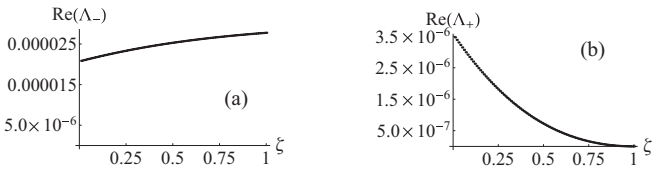

FIG. 7. Re(Λ) is plotted, for the two modes, as a function of the relative density ζ in the two shells in the shell-shell configuration. $\beta = 0.5$, $k_0R = 0.05$.

Its roots are given by

$$\mu_{\pm} = \tfrac{1}{6}(3 + \zeta \pm \sqrt{1 + 8\beta^3 + 2\zeta - 8\beta^3\zeta + \zeta^2}). \quad \text{(C9)}$$

We plot in Fig. 6 these analytic expressions for $\beta = \frac{1}{2}$ as a function of ζ and compare them with the same quantities numerically obtained by solving the Maxwell equation as described in Ref. [1] for $u_0 = 0.05$. We note that the two curves are indistinguishable. For the sake of completeness, we plot in Fig. 7 the corresponding numerical values for $\mathrm{Re}(\Lambda_s)$. As can be noted, as $\zeta \to 1$, giving uniform density, $\mathrm{Re}(\Lambda_-) \to \Lambda_{\mathrm{Dicke}} = \frac{2}{9}u_0^3$, while $\mathrm{Re}(\Lambda_+) \to 0$ (i.e., the pseudostate [11]).

[1] R. Friedberg and J. T. Manassah, Phys. Rev. A **85**, 013834 (2012).
[2] R. H. Dicke, Phys. Rev. **93**, 99 (1954).
[3] V. M. Fain, Sov. Phys. JETP **36**, 798 (1959).
[4] R. Friedberg, S. R. Hartmann, and J. T. Manassah, Phys. Lett. A **40**, 365 (1972).
[5] R. Friedberg, S. R. Hartmann, and J. T. Manassah, Phys. Rep. **7**, 101 (1973).
[6] R. Friedberg and S. R. Hartmann, Opt. Commun. **10**, 298 (1974); Phys. Rev. A **10**, 1728 (1974).
[7] S. Prasad and R. J. Glauber, Phys. Rev. A **82**, 063805 (2010).
[8] R. Friedberg and J. T. Manassah, Phys. Lett. A **372**, 6833 (2008).
[9] R. Friedberg and J. T. Manassah, Phys. Rev. A **81**, 063822 (2010).
[10] R. Friedberg, J. Phys. B **44**, 175505 (2011).
[11] R. Friedberg and J. T. Manassah, J. Math. Phys. **52**, 042107 (2011).